Semiempirical modeling free energy surfaces for proton transfer in polar aprotic solvents

ARTICLE *in* CHEMICAL PHYSICS · APRIL 2000

Impact Factor: 1.65 · DOI: 10.1016/S0301-0104(00)00045-8

4 AUTHORS:

Mikhail V Vener
Mendeleev Russian University of Chem…
69 PUBLICATIONS **1,186** CITATIONS
SEE PROFILE

Ivan Vladimirovich Rostov
Australian National University
21 PUBLICATIONS **329** CITATIONS
SEE PROFILE

Alexander V. Soudackov
University of Illinois, Urbana-Champaign
54 PUBLICATIONS **1,753** CITATIONS
SEE PROFILE

M. V. Basilevsky
Russian Academy of Sciences
108 PUBLICATIONS **1,713** CITATIONS
SEE PROFILE

ELSEVIER

Chemical Physics 254 (2000) 249–265

Chemical Physics

www.elsevier.nl/locate/chemphys

Semiempirical modeling free energy surfaces for proton transfer in polar aprotic solvents

M.V. Vener *, I.V. Rostov, A.V. Soudackov, M.V. Basilevsky

Karpov Institute of Physical Chemistry, ul Vorontsovo pole 10, 103064 Moscow, Russian Federation

Received 1 December 1999

Abstract

A method of calculation of a free-energy surface (FES) of the proton transfer (PT) reaction in a polar aprotic solvent is developed. This is based on the two-state (valence bond) VB description of the solute combined with recent continuum medium models. Its essential new feature is an explicit quantum-chemical treatment of VB wave functions, including internal electronic structure of a chemical subsystem. The FES includes a pair of intrasolute coordinates, R, the distance between hydrogen-bonded atoms and s, the proton coordinate, together with the collective medium polarization mode. Two hydrogen-bonded systems immersed in a polar solvent (Freon) were considered. The first one is the $H_5O_2^+$ ion, a model system which was used as a benchmark testifying the validity of our semiempirical calculations. The second system is the neutral $(CN)(CH_3)N–H\cdots N(CH_3)_3$ complex in Freon. PT for this system has been studied experimentally. The dependencies of basic parameters controlling FES properties (the overlap integral, the coupling matrix element and the reorganization energy E_r) on intrasolute coordinates R and s are evaluated and discussed. In particular, for the neutral complex, E_r depends on s linearly, and its dependence on R is weak. The FES, for the neutral system, has two potential wells separated by the energy barrier of $\sim$7 kcal/mol. Quantum-mechanical averaging over the proton coordinate, s, reduces the barrier from 7.0 to 1.2 kcal/mol. The value of the nonadiabatic parameter on the averaged FES is equal to 0.13. This implies that the PT in the second system corresponds to an intermediate dynamic regime and that proton tunneling effects are hardly significant for this reaction.

1. Introduction

Understanding at the microscopic level, interpretation and prediction of mechanisms and kinetics of proton transfer (PT) reactions in polar solvents is a challenging objective of contemporary research in theoretical chemistry [1–4]. A combination of nontrivial medium effects with an essentially quantum-mechanical character of a PT process makes this problem both difficult and important as a benchmark for developing and testifying various approaches.

Conventionally, a first step of a theoretical investigation of an elementary chemical process in solution involves a computation of its free-energy surface (FES) in space of chemical coordinates with the possible inclusion of solvent coordinates into consideration. This can be performed either at a true microscopic level within an MD simulation [5–13] or in terms of phenomenological continuum solvent models [7,8,14–18]. The first approach treating solvent effects at the most fundamental

* Corresponding author.
E-mail address: vener@cc.nifhi.ac.ru (M.V. Vener).

0301-0104/00/$ - see front matter
PII: S0301-0104(00)00045-8

level uses very simple models of solute electronic structure and, therefore, is now hardly appropriate for studies of real complex chemical objects. On the other hand, the continuum medium approach, which is computationally less restrictive and better compatible with conventional quantum-chemical packages, has certain advantages in this respect.

In a standard treatment of a collinear PT in H-bonded systems, the two most essential solute coordinates are introduced in the following way:

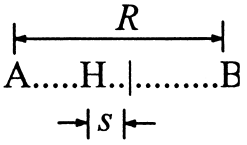

(1.1)

A and B represent terminal atoms of heavy molecular fragments R_A and R_B. The two PT variables shown schematically above are R, the distance between A and B, and s, the proton coordinate measured from the center of mass of the PT reaction center. Although an underlying quantum-chemical computation can treat to a full extent the internal electronic structure of molecular fragments R_A and R_B, their schematic representation in terms of two valence bond (VB) structures is required at the stage of introducing collective medium coordinates of continuum solvent models. There exist several levels of a VB scheme as implemented in the literature [7,8,14–24]. The most simple one applies the London–Eyring–Polanye–Sato (LEPS) approach as a convenient analytical formula to treat the gas-phase two-dimensional PT model (1.1). Here LEPS parameters are considered on purely empirical grounds to fit a quantum-chemical potential surface. More sophisticated approaches invoke an explicit two-state VB representation of a solute electronic structure at the stage of studying medium effects on PT processes. This is required to generate molecular charge distributions which underlie a reaction field computation in terms of a continuum theory. An importance of adding a third VB structure, namely that carrying a positive charge on the proton, has been emphasized [25]. This point is undoubtedly meaningful, and it is supported by results of the present work (see the discussion below). Still, because such an extension would significantly complicate a computational algorithm, the two-state model remains the most popular procedure for describing a PT in solution, although its overcontracted VB basis set brings in several inherent problems.

The main objective of the present work is to develop the two-state approach by its combining with recent continuum medium models [26–29] involving as an ingredient a consistent treatment of collective solvent coordinates [30–36]. Its essential new feature is an explicit quantum-chemical treatment of VB wave functions, including internal electronic structure of molecular fragments R_A and R_B. A more or less similar attempt to treat different (a more simple solute system) solution phase reaction has been reported [37,38].

The electron wave function of a PT system (1.1) is written as

$$\Psi = C_1\varphi_1 + C_2\varphi_2, \tag{1.2}$$

where coefficients C_1 and C_2 are found by means of a double diagonalization of the two-state Hamiltonian matrix,

$$H = \begin{pmatrix} H_{11} & H_{12} \\ H_{12} & H_{22} \end{pmatrix} \tag{1.3}$$

and the overlap matrix,

$$\Sigma = \begin{pmatrix} 1 & \sigma \\ \sigma & 1 \end{pmatrix}, \quad \sigma = \langle\varphi_1|\varphi_2\rangle. \tag{1.4}$$

The two VB basis functions are denoted as φ_1, φ_2.

Here all matrix elements are functions of R, s and a medium coordinate. The scheme proposed below suggests a consistent prescription for establishing this dependency. Including several empirical elements makes it sufficiently flexible for fitting desired FES properties. We implement this methodology for FES computations describing a PT in the reaction center (1.1) for a real H-bonded complex in a polar aprotic solvent.

The presentation of the material consists of two parts: the first methodological part (Sections 2–4 and Appendix A) describes a computational scheme and its underlying theoretical background. We tried to do this in a self-contained manner so that essential elements of reasoning and prescriptions could be available from the present text. The

second part, involving test calculations, further applications to real PT systems and a discussion of results, is contained in Sections 5–8 and Appendix B.

2. The gas-phase system

2.1. Gas-phase Hamiltonian and valence bond basis functions

Here the medium coordinate is absent. The Hamiltonian has the form,

$$h = \begin{pmatrix} h_{11} & h_{12} \\ h_{12} & h_{22} \end{pmatrix} \tag{2.1}$$

and we use conventional LEPS prescriptions [39] to evaluate the corresponding matrix elements.

This implies a specification of the electronic basis functions in Eq. (1.2) as two VB structures

$$\begin{array}{ll} \mathrm{A{-}H} \quad \mathrm{B} & (\varphi_1), \\ \mathrm{A^-\,H{-}B^+} & (\varphi_2) \end{array} \tag{2.2}$$

in which coordinates R and s are the same and fixed at some prescribed values. The actual evaluation of functions φ_1 and φ_2 includes, as a preliminary, an HF MO computation of four independent molecular fragments $\mathrm{R_A}$–H, $\mathrm{R_B}$, $\mathrm{R_A^-}$, and H–$\mathrm{R_B^+}$ with their geometries specified by given values of R and s. For a case considered here (neutral PT, system (1.1) is uncharged), all four fragments have closed electronic shells. At this stage, there is no limitation requiring to treat A and B as hard spheres; the quantum-chemical calculations were performed with real molecular fragments $\mathrm{R_A}$ and $\mathrm{R_B}$. Let us designate as ξ_{1v} ($v = 1, \ldots, N/2$) the $N/2$ lowest doubly occupied MOs obtained for the first structure in Eq. (2.2). Here N is the total number of electrons. Note that this set of MOs consists of two independent subsets. A similar set of MOs ξ_{2v} is calculated for the second structure in Eq. (2.2). Then, the overlap integral is calculated as

$$\sigma = \left[\det\left|\left\langle \xi_{1v} | \xi_{2\mu} \right\rangle\right|\right]^2 \tag{2.3}$$

where $|\ldots|$ means the $N/2 \times N/2$ matrix is built up of the corresponding matrix elements.

2.2. Orthogonalization

We perform Löwdin orthogonalization of the basis set (φ_1, φ_2):

$$(\lambda_1, \lambda_2) = (\varphi_1, \varphi_2)\Sigma^{-1/2}. \tag{2.4}$$

The overlap matrix Σ is defined in Eq. (1.4). This results in the orthogonalized Hamiltonian,

$$h^{(\lambda)} = \Sigma^{-1/2} h \Sigma^{-1/2} = \begin{pmatrix} \alpha_1 & \beta \\ \beta & \alpha_2 \end{pmatrix}. \tag{2.5}$$

Explicit expressions of the matrix elements are listed in Eq. (2.8) of Ref. [16].

2.3. The density matrix

We need an electron first-order transition density matrix for the system of wave functions (2.2):

$$\rho^{(g)} = \begin{pmatrix} \rho_{11}^{(g)} & \rho_{12}^{(g)} \\ \rho_{12}^{(g)} & \rho_{22}^{(g)} \end{pmatrix}. \tag{2.6}$$

The diagonal quantities $\rho_{11}^{(g)}$ and $\rho_{22}^{(g)}$ are calculated in terms of the AO coefficients corresponding to MOs ξ_{1v} and ξ_{2v} following standard prescriptions [40]. According to the procedure accepted in this section, the mutual polarization of fragments "1" and "2" as well as their polarization by the solvent reaction field is neglected. For the off-diagonal term, we assume

$$\rho_{12}^{(g)} = \frac{\sigma}{2}\left(\rho_{11}^{(g)} + \rho_{22}^{(g)}\right). \tag{2.7}$$

The orthogonalized density matrix $\rho^{(\lambda)} \equiv \rho$ is then obtained as

$$\rho = \Sigma^{-1/2}\rho^{(g)}\Sigma^{-1/2} + \rho_n = \begin{pmatrix} \rho_{11} & \rho_{12} \\ \rho_{12} & \rho_{22} \end{pmatrix}, \tag{2.8}$$

where the matrix elements are

$$\begin{aligned} \rho_{11} &= \frac{1}{2}\left(\rho_{11}^{(g)} + \rho_{22}^{(g)}\right) + \frac{\rho_{11}^{(g)} - \rho_{22}^{(g)}}{2\sqrt{1-\sigma^2}} + \rho_n, \\ \rho_{22} &= \frac{1}{2}\left(\rho_{11}^{(g)} + \rho_{22}^{(g)}\right) - \frac{\rho_{11}^{(g)} - \rho_{22}^{(g)}}{2\sqrt{1-\sigma^2}} + \rho_n \end{aligned} \tag{2.9}$$

and

$$\rho_{12} = \rho_{21} = 0. \tag{2.10}$$

The quantity ρ_n in Eqs. (2.8) and (2.9) represents the nuclear charge distribution. Result (2.10) is a consequence of our assumption (2.7). Alternatively, we could postulate the condition $\rho_{12} = 0$ and then, Eq. (2.7) would follow. We invoke the present approximation in order to avoid a cumbersome procedure of an explicit evaluation of $\rho_{12}^{(g)}$ in a nonorthogonal basis [40,41].

2.4. The LEPS correction function

A modification of the LEPS potential is required in order to describe the gas-phase potential of the H-bonded complex in a qualitatively correct manner. This is gained by adding a scalar function $G(R)$ to the Hamiltonian (2.5). The function is defined as

$$G(R) = (1/2)K_{\mathrm{harm}}(R - R_0)^{**}2, \tag{2.11}$$

where K_{harm} and R_0 are adjustable parameters. This creates a potential well along the heavy atom coordinate R.

3. The solution-phase system

The construction of FESs explicitly depending on medium coordinates follows the general scheme elaborated earlier [32,33]. This consists of several steps.

3.1. Continuum medium calculations

The present approach is based on a linear response treatment postulating the linear relation between the charge density ρ_{ab} and the medium response field Φ_{ab} (the reaction field):

$$\begin{aligned} \Phi_{ab} &= \hat{K}\rho_{ab}, \\ \Phi_{ab}^{(\infty)} &= \hat{K}_\infty \rho_{ab}, \\ \Phi_{ab}^{(\mathrm{in})} &= \left[\hat{K} - \hat{K}_\infty\right]\rho_{ab} \equiv \hat{K}_{\mathrm{in}}\rho_{ab}, \end{aligned} \tag{3.1}$$

where a and b run over all number of basis states taken onto account. The linear integral operators $\hat{K}$ and $\hat{K}_\infty$ are not known explicitly, but their matrix elements can be computed in terms of various solvation models. For the case of dielectric continuum solvent models with the explicit account of solute excluded volume, the calculation reduces to a numerical solution of two-dimensional integral equations [27–29] for the charge density on the surface of a cavity in which a solute system is immersed. Operators $\hat{K}$ and $\hat{K}_\infty$ correspond to the calculations in which the continuum solvent is characterized by two dielectric constants equal to ε_0 (the static dielectric constant) and ε_∞ (the optical dielectric constant), respectively. They represent the total and optical medium responses; the operator $\hat{K}_{\mathrm{in}}$ represents the response corresponding to the inertial (mainly orientational) polarization field. In the most advanced frequency resolved cavity model (FRCM) scheme [29] both ε_0 and ε_∞ are involved in a computation of $\hat{K}$ but the further prescription for separation of $\Phi_{ab}^{(\mathrm{in})}$ follows Scheme (3.1) [42].

3.2. Reorganization matrices

The main outcome of a continuum model calculation are the so-called reorganization matrices with the elements

$$\begin{aligned} T_{ab,a'b'}^{(\infty)} &= -\int \mathrm{d}^3 r\, \rho_{ab}\hat{K}_\infty \rho_{a'b'}, \\ T_{ab,a'b'}^{(\mathrm{in})} &= -\int \mathrm{d}^3 r\, \rho_{ab}\hat{K}_{\mathrm{in}}\rho_{a'b'} \equiv T_{ab,a'b'} \end{aligned} \tag{3.2}$$

(we suppress, for brevity, superscript "in" hereafter). With off-diagonal densities ρ_{ab} satisfying Eq. (2.10), we deal with two-dimensional matrices ($ab = 11, 22$):

$$\begin{aligned} T_\infty &= \begin{pmatrix} T_{11,11}^{(\infty)} & T_{11,22}^{(\infty)} \\ T_{11,22}^{(\infty)} & T_{22,22}^{(\infty)} \end{pmatrix} \quad \text{(electronic)}, \\ T &= \begin{pmatrix} T_{11,11} & T_{11,22} \\ T_{11,22} & T_{22,22} \end{pmatrix} \quad \text{(inertial)}. \end{aligned} \tag{3.3}$$

3.3. The CI/BO 2 × 2 Hamiltonian

The orthogonalized two-state Hamiltonian $H^{(\lambda)}$, including medium polarization effects, has the form of Eq. (1.3). In its construction, the matrix elements of orthogonalized Hamiltonian $h^{(\lambda)}$ (2.5) are used as building blocks:

$$H_{aa} = \alpha_a + U_{aa}^{(\infty)} + Y_{aa}, \quad a = 1,2. \\ H_{12} = \beta. \tag{3.4}$$

We suppressed superscript λ for brevity.

The last two terms in the diagonal elements represent solvent effects. The first one is an equilibrium solvent potential (different for two different states) due to the electronic (optical) polarization. It is generally evaluated as [33]

$$U_{ab}^{(\infty)} = -\frac{1}{2}\sum_c T_{ac,cb}^{(\infty)}. \tag{3.5}$$

This result corresponds to the so-called CI/BO approximation for medium electrons [33,36, 37,43,44]. For the present case with condition (2.10),

$$U_{aa}^{(\infty)} = -\frac{1}{2}T_{aa,aa}^{(\infty)}. \tag{3.6}$$

The two solvation terms Y_{11} and Y_{22} in Eq. (3.4) represent a pair of solvation coordinates formally defined as

$$Y_{aa} = \int \mathrm{d}^3 r\, \Phi_{\mathrm{in}} \rho_{aa}, \tag{3.7}$$

where Φ_{in} is the inertial response field, a three-dimensional continuum variable describing non-equilibrium solvation effects.

3.4. The free energy surface in terms of coordinates Y_{11}, Y_{22}

The two (ground and excited state) FESs of the two-state PT model are constructed by adding the polarization self-energy S to the eigenvalues of Hamiltonian H (Eqs. (1.3) and (3.4)) [32,33]. These eigenvalues are denoted as W_1, W_2, whereas the expression for S is

$$S(Y_{11}, Y_{22}) = \frac{1}{2}\Big[\big(T^{-1}\big)_{11,11} Y_{11}^2 + \big(T^{-1}\big)_{22,22} Y_{22}^2 + 2\big(T^{-1}\big)_{11,22} Y_{11} Y_{22}\Big]. \tag{3.8}$$

Thereby, the two FESs are

$$U_a(Y_{11}, Y_{22}) = W_a + S(Y_{11}, Y_{22}). \tag{3.9}$$

Their dependence on the solute coordinates R and s is suppressed in this notation.

3.5. Reduction of the number of variables

We first perform a transformation of medium coordinates as

$$Z_{11} = Y_{11}, \\ Z_{22} = Y_{22} - Y_{11} \equiv Z. \tag{3.10}$$

The corresponding transformation of the reorganization matrix T reads

$$T' = \begin{pmatrix} T'_{11,11} & T'_{11,22} \\ & T'_{11,22} T'_{22,22} \end{pmatrix}, \\ T'_{11,11} = T_{11,11}, \\ T'_{22,22} = T_{11,11} + T_{22,22} - 2T_{11,22}, \\ T'_{11,22} = T_{11,22} - T_{11,11}. \tag{3.11}$$

Transformation (3.10) keeps invariant [33] the FES expression (3.9), so

$$U_a(Z_{11}, Z_{22}) = W_a + S(Z_{11}, Z_{22}), \tag{3.12}$$

where W_1 and W_2 are now considered as functions of Z_{11}, Z_{22}, and S is calculated as a quadratic form in terms of matrix $(T')^{-1}$ and variables Z_{11}, Z_{22}, similar to Eq. (3.8).

The crucial step in the following reduction procedure is an introduction of the reduced Hamiltonian (I is the unit matrix):

$$\overline{H} = H - Y_{11} I. \tag{3.13}$$

Its eigenvalues

$$\overline{W}_a = W_a - Y_{11} \tag{3.14}$$

are independent of Y_{11}; they depend only on coordinate $Z = Y_{22} - Y_{11}$. The reduced one-dimensional FESs $U_{1,2}(Z)$ have the form ($a = 1,2$):

$$U_a(Z) = \overline{W}_a(Z) + \frac{1}{4E_{\mathrm{r}}}(Z + T_{11,22} - T_{11,11})^2 - \frac{1}{2}T_{11,11}. \tag{3.15}$$

Here

$$E_{\mathrm{r}} = \frac{1}{2}T'_{22,22} \tag{3.16}$$

is the inertial solvent reorganization energy associated with the coordinate Z.

A possibility of a complete elimination of first variable Y_{11} is demonstrated in Appendix A. It is important to emphasize here that FESs (3.15) and (3.12) are completely equivalent only at stationary points (minima and saddles) of the ground state two-dimensional FES $U_1(Z_{11}, Z_{22})$. The full coincidence is disturbed at other points. This is the price to be paid for the advantage of having a single medium coordinate.

3.6. The four-level scheme

The four-level theory [43,44] is an attempt to circumvent the limitation of the CI/BO approximation for medium electrons invoked in Section 3.3. This approximation treats the electronic polarization as an infinitely fast quantum variable and results in an operator (or matrix, see Eq. (3.5)) form of the potential $U^{(\infty)}$ which it creates for the motion of slow orientational coordinates Y_{11}, Y_{22} (or Z_{11}, Z_{22}). Such an approach is quite different from the equilibrium treatment of the usual SCRF theory, where electronic polarization is considered classically: it adjusts to given positions of orientational coordinates, producing a single potential function. Therefore, equilibrium solvation calculations in terms of CI/BO and SCRF techniques give different results. For instance, the CI/BO calculation discards the effect of medium electronic polarization on the energy at the FES saddle point, which is present in a SCRF calculation [36]. The four-level theory bridges between these two extremes which are identified as two of its limiting cases when the basic solvent parameter

$$\sigma_{\mathrm{solv}} = \exp\left(-\frac{R_\infty}{\hbar\omega_{\mathrm{el}}}\right) \tag{3.17}$$

tends either to 1 (the CI/BO limit) or to 0 (the SCRF limit). (This SCRF limit corresponds to a 2×2 CI wave function. The HF SCRF limit is obtained in a different procedure [33].) Here R_∞ is the solvent electronic reorganization energy, a counterpart of the corresponding inertial quantity (Eq. (3.16)). It is defined as

$$R_\infty = \frac{1}{2}\left(T^{(\infty)}_{11,11} + T^{(\infty)}_{22,22} - 2T^{(\infty)}_{11,22}\right), \tag{3.18}$$

whereas $\hbar\omega_{\mathrm{el}}$ is an empirical quantity mimicking a first electronic excitation in the bulk solvent [36]. We address the reader to the original literature [36,43,44] for a full description of a four-level calculation.

3.7. The electron/proton double adiabatic model and its limits

At this stage, we proceed to the three-dimensional PT FES $U(s,R,Z)$ constructed as described above. This was called "LEPS-3" in our preceding works [16,45]. Following the earlier developed methodology [6–8,16,45], it has to be further averaged over the fast proton motion by solving a one-dimensional Schrödinger equation for coordinate s with fixed coordinates R and Z. In the adiabatic kinetic regime, the resulting two-dimensional FES, called "FES-2", governs the motion of the two heavy coordinates, which is considered as purely classical; hence, its kinetic treatment is more or less evident. The averaging procedure stands as an alternative method to allow for the proton tunneling on LEPS-3. It generally overestimates the tunneling. A more adequate approach is formulated in terms of a pair of averaged two-dimensional adiabatic FESs, separated by the energy gap Δ and coupled by the matrix element $\langle G_{12}\rangle_{\mathrm{T}}$; both these quantities are functions of R and Z. The main nonadiabatic effect in the PT kinetics arises as a reflection of the reactive flux in the region of avoided crossing. Sometimes, it can be strong, producing extremely small transmission factors [45]. A simple way to learn whether this is important or not is to compute the ratio $\langle G_{12}\rangle_{\mathrm{T}}/\Delta$ at the transition state of the FES-2 and inquire whether it is large or small (as compared to 1). Such a test concludes the present study aimed at giving a primary qualitative picture of the PT kinetics.

4. The computational details

The actual computation of the FESs consists of generating the Hamiltonian matrix elements α_{aa}, β and σ (Eqs. (2.3) and (2.5)) and reorganization matrices T_∞ and $T_{\mathrm{in}} \equiv T$ (Eqs. (3.2) and (3.3)) as

functions of solute coordinates R and s. Important quantities governing solvation effects are reorganization energies E_r (Eq. (3.16)) and R_∞ (Eq. (3.18)) and electronic solvation energies $U_{aa}^{(\infty)}$ (3.6). Note also the quantity $T_{11,11}$ in Eq. (3.15). It could be ignored (as a trivial constant) in earlier electron transfer studies [33,34], but in the present PT case, it affects, as a function of R and s, the total FES. All solvation computations followed the FRCM scheme [29,30] with a parameterization specified below. In this method, the solute system is surrounded by two cavities constructed in terms of overlapping spheres drawn around each of solute atoms, as in the original PCM procedure [26,27]. The dielectric constant is $\varepsilon = 1$ within the inner cavity. An optical value $\varepsilon = \varepsilon_\infty$ works between two surfaces. Finally, the outside of the outer cavity has $\varepsilon = \varepsilon_0$ (the static dielectric constant) for total polarization field or $\varepsilon = \varepsilon_\infty$ when only the fast electronic part is taken into account. The radii of interlocking spheres are chosen as

$$\begin{aligned} r_{1i} &= \kappa R_{\mathrm{vdWi}} \quad \text{(inner cavity)}, \\ r_{2i} &= r_{1i} + \delta \quad \text{(outer cavity)} \end{aligned} \tag{4.1}$$

where for each solute atom i R_{vdW} is its van der Waals radius; κ and δ are FRCM parameters. For a given pair (R, s), we calculated MOs ξ_{1v} and ξ_{2v} (see Section 2.1) within a PM3 method [46] and used them to calculate the overlap integral (2.3) and orthogonalized charge densities (2.9), which also contained a nuclear charge density component. An FRCM calculation was then monitored to generate reorganization matrices T_∞ and T (Eq. (3.3)). All systems in the present study were treated in solution of CHF_2Cl:CHF_3. The values of the parameters which were used to describe electrostatic properties of the solvent [47] are given in Table 5. The solute–solvent interface was being constructed of two different size molecular shape cavities setting boundary conditions for inertial and inertialess modes of polarization of solvent [29,42]. Unfortunately, the solvent considered in this study is not parameterized in the FRCM model. This gives rise to a question about the parameter δ in Eq. (4.1) that sets a thickness of layer with a lower dielectric constant between the cavities. As was mentioned by the authors of the FRCM model [30], δ has a rough correlation with the physical size of a solvent molecule. Thus, the value $\delta = 1.1$ was chosen to build the outer cavity around the solute. This value corresponds to methanol, whose molecular size was considered to be quite close to CHF_2Cl and CHF_3. Another FRCM parameter is solvent independent, and it was set to 0.9 according to a general prescription [30].

5. The PT systems

We considered two hydrogen-bonded systems immersed in a polar aprotic solvent. The first system is the $H_5O_2^+$ ion, this complex is widely used in the literature as a model PT system, e.g. see Ref. [48]. It should be stressed that PT is not observed in this complex since the potential FES of the ion has only one minimum in the gas phase [49–51] and polar solvents [52–54]. By fixing the O···O distance at the values which are larger than the equilibrium one (~2.4 Å), a symmetrical double-well potential along the proton coordinate can be obtained. Due to the symmetry and simplicity of this system, this will be used below as a benchmark testifying the validity of our semiempirical computations.

The second system is the neutral $(CN)(CH_3)N$–$H\cdots N(CH_3)_3$ hydrogen-bonded complex. This will be referred below as an "acid–base" complex (ABC). Recently, PT for this system in a polar solvent has been studied experimentally (low-temperature NMR techniques) and theoretically (the ab initio/self-consistent reaction field (SCRF) level of computation) [47]. The PT rate and H/D isotope effect were measured within the temperature interval 100–150 K in a mix of Freons CHF_2Cl:CHF_3 (1:1). The PT rate increases from 300 s^{-1} at 110 K to 7000 s^{-1} at 150 K. The H/D isotope effect is 2.8 at 150 K and decreases with decreasing temperature. The free energy of the reaction is of the order of k_BT, while the activation energy is ~2.5 kcal/mol. The Arrhenius plot is nonlinear. The reaction rate pre-factor is much less than 10^{13} s^{-1}.

In the present preliminary report, we expose and discuss the dependencies on intrasolute

coordinates R and s of basic parameters controlling FES properties of these systems, such as overlap integral σ (Eq. (2.3)), the coupling matrix element β (Eq. (2.5)) and the reorganization energy E_r (3.16).

6. Results

6.1. The gas-phase calculations

Calculations of the electronic structure of two H-bonded systems have been performed using the semiempirical PM3 method. Their gas-phase potentials were fitted by the LEPS-type function. Optimum LEPS parameters obtained for both systems are listed in Table 1. The values of the LEPS correction function, see Eq. (2.11), are also shown in Table 1.

6.1.1. The $H_5O_2^+$ ion

The gas-phase potential energy surface of this complex has only one minimum (the transferred proton locates at the midpoint between the oxygen atoms). The equilibrium O···O distance is approximately 2.40 Å and the O–H···O fragment is slightly nonlinear. The absolute value of the overlap integral σ for the ion is ~0.5. Its maximum value occurs at the midpoint between the heavy atoms and decreases while the proton shifts to the oxygen atom. This dependence is caused by the variation of charge of the transferred proton while it shifts from one oxygen to the other. The proton has a maximum charge of +0.46 a.u. (i.e. it is most strongly deshielded) at the midpoint between the heavy atoms ($s = 0$). Its charge falls down to +0.3 a.u. when it becomes localized near the oxygen atom. The value of charge is less sensitive to the variation of the R coordinate. The absolute value of σ is sensitive to the s variation, while its dependence on R is weak.

Table 1
Optimum LEPS parameters[a] for the $H_5O_2^+$ ion and the ABC in gas phase

	$H_5O_2^+$ ion	ABC
D_{AH}, kcal/mol	88.0	90.0
D_{BH}, kcal/mol	88.0	47.0
D_{AB}, kcal/mol	8.8	7.8
r_{AH}, Å	1.0	1.0
r_{BH}, Å	1.0	1.1
r_{AB}, Å	2.7	2.5
β_{AH}, Å^{-1}	2.60	2.32
β_{BH}, Å^{-1}	2.60	2.25
β_{AB}, Å^{-1}	1.69	1.69
K_{AH}	0.55	0.90
K_{BH}	0.55	0.05
K_{AB}	0.2	0.325
K_{harm}, kcal/mol Å^{-2}	–	200
R_0, Å	–	5.4

The values of the LEPS correction function, see Eq. (2.11), are also given for the ABC.

[a] For a definition of parameters, see Eqs. (2.8) and (5.5) in Ref. [16].

The absolute value of β in the $H_5O_2^+$ ion is less than 2 kcal/mol. When the proton locates at the midpoint between oxygens, it becomes less than 0.3 kcal/mol. In order to interpret this result, one has to consider the dependence of β on the parameters of the gas-phase Hamiltonian, see Eq. (2.5) in the present paper and paragraph 2 in Ref. [16]. It is easy to show that

$$\beta \sim \frac{3}{2}J_{AB} - \frac{3}{4}J_{AH} - \frac{3}{4}J_{BH}. \tag{6.1}$$

Here J_{ij} is the exchange integral, depending on the LEPS parameters (Table 1) via singlet bonding and triplet antibonding Morse potentials for pair of atoms i and j, see Eqs. (5.6a) and (5.6b) in Ref. [16]. For the symmetric $H_5O_2^+$ system $\frac{3}{2}J_{AB} \approx \frac{3}{2}J_{AH}$ and β turns out to be very small, especially when the proton locates at the midpoint between oxygens. β depends on both intrasolute coordinates; however, the dependence on R is much weaker, than on s, due to the difference in the breaking energies of the A···B and A–H bonds (parameters D_{AB} and D_{AH} respectively, see Table 1).

6.1.2. The acid–base complex

The gas-phase PES of ABC has only one minimum which corresponds to the reactant species (the transferred proton locates near nitrogen atom of the "acid" fragment). The equilibrium N···N distance (R_e) is equal to 2.877 Å and the N–H···N fragment is slightly nonlinear. The PM3 potential energy profile as a function of s at the fixed R_e distance is given in Fig. 1. (It should be noted that

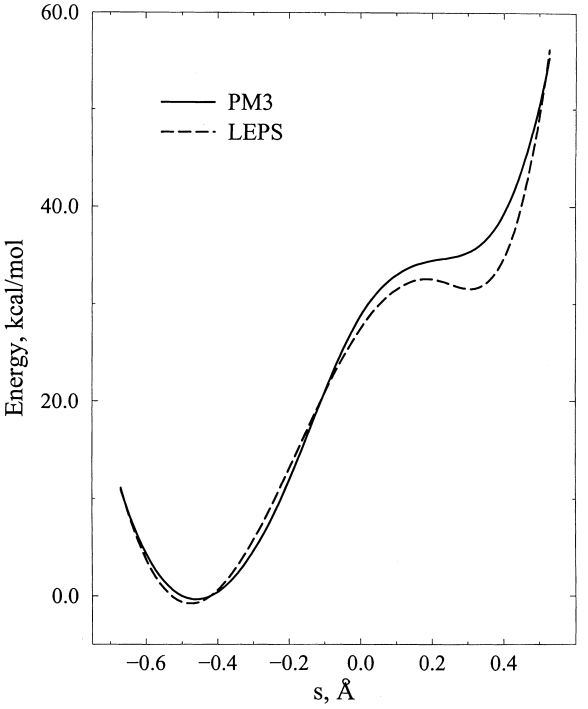

Fig. 1. The cross-sections of the PM3 gas-phase potential (—) and the corresponding LEPS function (– – –) of the ABC complex at $R = 2.877$ Å (the equilibrium N···N distance).

these results agree fairly well with those obtained at the MP2/6-31G(d) level of computation [47]). The cross-section of the LEPS function is also given in Fig. 1. These results are further discussed in Section 7.

The value of the overlap integral σ varies around 0.3. σ is sensitive to a variation of the s coordinate, while its dependence on R is weak. It decreases while proton shifts from the "acid" partner ($\sigma = 0.34$) to the "base" one ($\sigma = 0.26$) at the equilibrium N···N distance. This dependence is caused by the strong variation of charge on the transferred proton with the s variation. When the proton locates near the "acid" partner, its charge is 0.65 a.u., whereas near the "base" partner, it is 1.0 a.u.

For the ABC, the absolute value of parameter β is large (>30 kcal/mol). In terms of Eq. (6.1), this can be explained in the following way. Due to the asymmetry of the ABC potential in the gas phase, see Fig. 1, the breaking energies of the A–H and B–H bonds differ drastically, see Table 1. This implies that the last term in Eq. (6.1) can be omitted and β turns out to be much larger, than in the case of $H_5O_2^+$. β does depend on both intrasolute coordinates; however, due to the large absolute value of β, this dependence is not significant for the ABC.

According to our calculations, the value of the overlap integral relates closely to the charge on the transferred proton. For the "bare" proton, this value is less than 0.5. The β value depends on the parameters of the LEPS function in a rather complex way. Its absolute value relates closely to the symmetry of the gas-phase potential. In the asymmetric case, β is expected to have much larger values, than in the symmetric one.

6.2. PM3/SCRF calculations

Elements of reorganization matrices for both H-bonded complexes were calculated for cross-sections of the corresponding FESs along the collective medium coordinate Z for several fixed R values. In these computations, all intrasolute parameters were frozen at their equilibrium gas-phase values while proton was transferred from one H-bonded atom to another. The shape and volume of cavities surrounding the solute system were kept unchanged while proton shifted at fixed R.

6.2.1. The $H_5O_2^+$ ion

The absolute values of matrix elements $T_{11,11}$, $T_{11,22}$ and $T_{22,22}$ of electronic and inertial reorganization matrices (Section 3) were found to be of the same order of magnitude for the ion. Variations of all matrix elements with the s variation (at a given R value) are significant. The following symmetry identities hold:

$$T_{11,11}(s,R) = T_{22,22}(-s,R), \tag{6.2}$$

$$T_{11,22}(s,R) = T_{11,22}(-s,R). \tag{6.3}$$

The value of the reorganization energy was found to be very sensitive to both intrasolute

coordinates. Due to the symmetry of the system, it can be expressed as

$$E_r(s,R) = A_0(R) - A_2(R)^* s^* s. \quad (6.4)$$

In accordance with the Marcus prescription [55], the A_0 value decreases with an increase of R. The same is true for the A_2 coefficient. For instance, $A_0 = 6.2$ kcal/mol and $A_2 = 11.6$ kcal/mol Å^{-2} at $R = 2.70$ Å. A strong dependence of E_r on the proton coordinate can be easily explained if one takes into account the charge on the transferred proton as a function of s at the given R coordinate, see Section 6.1.

6.2.2. The acid–base complex

In contrast to the $H_5O_2^+$ ion, the absolute values of matrix elements $T_{11,11}$, $T_{11,22}$ and $T_{22,22}$ of electronic and inertial reorganization matrices in the ABC differ strongly from each other. The following is unequally valid for both matrices:

$$T_{11,11} < T_{11,22} \ll T_{22,22}. \quad (6.5)$$

The variation of $T_{11,11}$ is negligible, and it may be treated as constant. Other elements depend on s linearly, although their dependence on R is weak. As a result, the reorganization energy $E_r(s,R)$ depends on s linearly:

$$E_r(s,R) = A_0(R) + A_1(R)^* s. \quad (6.6)$$

The dependence of both coefficients on R is weak. The E_r value was found to be ~9 kcal/mol when a proton locates at the midpoint between heavy atoms ($s = 0$). The basic parameters controlling FES properties of the two systems are given in Table 2.

Table 2
Basic parameters controlling FES properties of two systems[a]

	σ	β (kcal/mol)	E_r (kcal/mol)
$H_5O_2^+$ ion	0.5	2	6
ABC	0.3	30	9

[a] All values are given for $s = 0$ and $R = R_e$, the equilibrium R value of the corresponding complex in gas phase.

6.3. The shape of the free-energy surface profiles along the medium coordinate

In the simplest version of the electron-transfer theory, the crucial role plays the quantity (e.g., see Ref. [35])

$$\zeta = |2\beta/E_r|, \quad (6.7)$$

where β is the off-diagonal matrix element (a parameter of the electronic coupling), see Eq. (2.5), and E_r is the solvent reorganization energy, see Eq. (3.16). It should be noted that the value of β comes from gas-phase calculations (we neglect its solvent dependence). In a symmetric system, if $\zeta > 1$, there exists a single-well free-energy profile, if $\zeta < 1$, a double-well curve appears along the collective medium coordinate Z.

The absolute value of β in the $H_5O_2^+$ ion is less than E_r when proton locates at $s = 0$ (Table 2). Therefore, the shallow double-well curve appears along the solvent coordinate in the vicinity of the mid-point $s = 0$. The value of β increases rapidly while the proton shifts to the oxygen atom and the cross-sections along the solvent coordinate have only one minimum when the proton shifts to one of the "heavy" atoms.

The absolute value of β in the ABC is much larger than E_r for all values of s and R, see Table 2. Therefore, FES profiles have only one minimum along Z.

Two- and four-level schemes of treating the electronic polarization (Section 3.6) give practically identical results for the $H_5O_2^+$ ion (this is a consequence of the small value of β) and very similar results for the ABC. The shapes of cross-sections along the solvent coordinate as well as the barrier height on the resultant FES for the ABC are similar for both schemes (only a slight shift on the energy axis is observed).

6.4. The free-energy surface of the acid–base complex

Calculated values of matrix elements $T_{11,11}$, $T_{11,22}$ and $T_{22,22}$, see Section 3 and Eq. (6.5), and the overlap integral σ, see Eq. (2.3), as functions of s and R, were used to generate the FES (LEPS-3) for the ABC. The PM3/SCRF characteristics of

Table 3
The PM3/SCRF parameters of the LEPS-3 function of the ABC

	A_0[a]	A_1	A_2
σ	0.31	−0.064	−0.05
$T^{\infty}_{11,11}$	3.1	0	0
$T^{\infty}_{11,22}$	6.4	3.8	0
$T^{\infty}_{22,22}$	12.0 (62.0)[b]	22.0	0
$T_{11,11}$	0.9	0	0
$T_{11,22}$	2.3	1.1	0
$T_{22,22}$	22.0	6.5	0

The elements of reorganization matrices are in kcal/mol.
[a] All parameters were approximated as $A_0 + A_1^* s + A_2^* s^* s$, where s is in Å.
[b] The result of the original computations is given in parentheses; the main figure is obtained by scaling, see the text.

the LEPS-3 function are given in table 3. Relative energies, the N···N and N–H distances and the value of the medium coordinate Z for the stationary structures of the PT process in the ABC are given in Table 4. These data were obtained by means of a special variation of parameters of LEPS, of the correction function (2.11) and the interpolation parameter A_0 of $T_{22,22}$ (Table 3). Details are discussed in Section 7.2. The important peculiarity of the LEPS-3 surface is relatively deep potential wells which correspond to the reactant and product species arranged at approximately the same energy level and separated by the energy barrier of ~7 kcal/mol. The reaction coordinate at the TS point (the decay mode) coincides with the s-motion. The cross-sections of LEPS-3 surface along R and Z represent single-well potentials.

Quantum-mechanical averaging LEPS-3 was performed by solving one-dimensional s-dependent Schrödinger equation [45] for given pairs of heavy-particle coordinates R and Z. Most interesting characteristics of the ground-state electron–proton FES-2 are given in Table 4. Averaging over the proton coordinate reduces the barrier from 7.0 to 1.2 kcal/mol and shifts the TS along the R-direction. Both effects were observed earlier for PT in the [C···H···C]-reaction center [45]. The relative stability of the reactant and product species does not change. An important characteristic of the FES-2 surface is the energy gap Δ between two lowest adiabatic electron–proton states at the TS point. Δ equals to 0.5 kcal/mol.

In order to verify the applicability of the double-adiabatic concept for the considered system, we estimated the value of the nonadiabatic parameter ξ [45],

$$\xi = \left| \frac{\langle G_{12} \rangle_T}{\Delta} \right|. \tag{6.8}$$

The procedure of evaluating the thermally averaged coupling matrix element $\langle G_{12} \rangle_T$ is described in Appendix B. For the ABC system, ξ is equal to 0.13. This value implies that we deal with an almost adiabatic dynamics on the FES-2. It should be noted that the computation of the coupling matrix element by applying a continuum solvent approximation as given in Appendix B is open to criticism, especially at its point regarding the estimate of the mass corresponding to the solvent coordinate, see Eq. (B.1). By varying this parameter to a reasonable extent, we were able to increase the nonadiabatic coupling up to $\xi = 0.6$ which shows that the dynamical interaction between the two surfaces could be hardly negligible. At least, we can conclude that this coupling is neither large nor extremely small so that the PT process proceeds either almost adiabatically or in an intermediate dynamic regime. In terms of the

Table 4
Relative energies ΔE, the N···N and N–H distances and the value of the medium coordinate Z for the stationary structures of PT in ABC before (LEPS-3) and after (FES-2) averaging over the s coordinate

	LEPS-3			FES-2		
	Reactant	TS	Product	Reactant	TS	Product
ΔE, kcal/mol	0	7.0	0.9	0	1.2	0.3
Z, kcal/mol	−9.5	−20.5	−27.5	−11.0	−20.0	−28.0
N···N, Å	2.84	2.75	2.86	2.82	2.84	2.85
N–H[a], Å	1.03	1.35	1.75	–	–	–

[a] The N–H distance between the "acid" nitrogen atom and the transferred proton.

dynamics on LEPS-3, this corresponds to the case when tunneling effects are not significant.

7. Comments and discussion

7.1. Parameterization of the valance bond/PM3 results

As a basic result of a computation outlined in Sections 2 and 3, we obtain reorganization matrices T_∞ and T (altogether six independent quantities) and the VB overlap integral σ. These seven parameters are functions of solute coordinates R and s. For the further purpose of computing FES-2 by quantum-mechanical averaging of the LEPS-3 surface, their values over fine grid of points are required. Actually, we used VB computations on a coarse-grained grid (the step 0.2 Å for R and 0.15 Å for s) as a background for the following interpolation. A possibility of linear or quadratic smoothing over s was revealed in preliminary tests (see Section 6.2). Note that such dependencies are essentially different in different PT systems such as the $H_5O_2^+$ ion and the ABC.

7.2. Fitting the energy profiles for acid–base complex

As usually, extended quantum-chemical computations and experimental evidence served as a test of validity for the semiempirical LEPS-3 surface. Most informative are its profiles along the proton coordinates s. Several general criteria can be formulated:

(a) Gas-phase profiles represent single-well potentials with a strongly anharmonic behavior (the shoulder) in the product range of s, corresponding to the VB structure φ_2. This is known from experimental studies of H-bonded systems [56–58] supported by ab initio calculations [59,60]. For the present ABC system, some benchmark results are reported elsewhere [47].

(b) The equilibrium N···N distance for the reactant minimum in solution is almost the same as in the gas phase [47].

(c) Profiles in solution within essential range of R represent double-well curves. The energies of their minima when computed with equilibrated medium coordinates are expected to be the same within 1–2 kcal/mol; the barrier height computed at the saddle point with relaxed medium is 7 kcal/mol [47].

Conditions (a) and (b) could be satisfied by fitting LEPS parameters and the correction function (2.11), see Table 1. Some results are illustrated by Figs. 1 and 2. Fitting the gas-phase profile was successful for equilibrium gas phase value R; for larger R significant deviations in the product region of s could not be avoided. It proved to be even more difficult to satisfy condition (c). The rigid procedure of computing VB charge densities and T matrices as specified above did not allow for fitting. As a result, we observed a strongly asymmetric three-dimensional surface. Its deep minimum was located in the product region, indicating

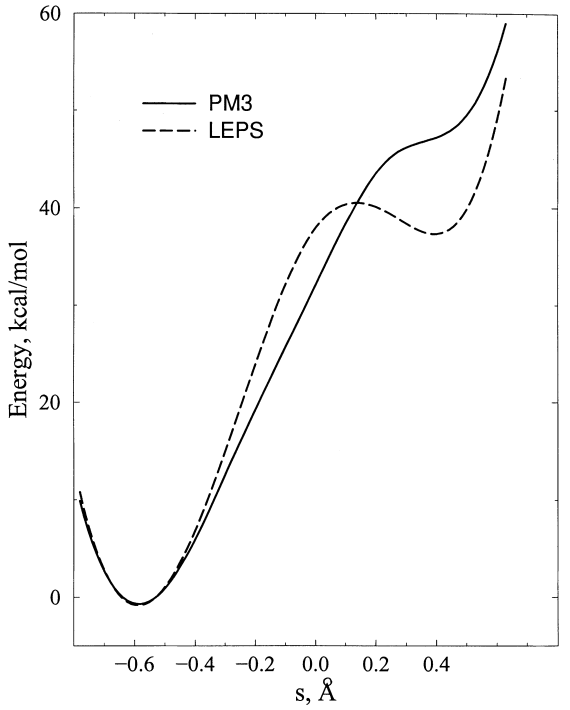

Fig. 2. The cross-sections of the PM3 gas-phase potential (—) and the corresponding LEPS function (– – –) of the ABC complex at $R = 3.1$ Å.

Table 5
The data used and computed for Freon (CHF_3) and bromoethane (C_2H_5Br)

CHF_3			C_2H_5Br		
Parameter	Its value	T, reference	Parameter	Its value	T, reference
ε_0	40	110 K, [47]	τ, s	4.2×10^{-12}	300 K, [63]
ε_∞	2	110 K, [47]	η, poise	37×10^{-3}	300 K, [62]
τ, s	7×10^{-11}	110 K, this work	η, poise	1.87×10^{-2}	160 K, [62]
ω_{eff}^2, s^{-2}	1.4×10^{25}	110 K, this work[a]	τ, s	7×10^{-11}	160 K, this work
μ_y, s^2	4.7×10^{-23}	This work			

[a] The value of effective rotational frequency of the Freon (we used gas-phase estimate) calculated from the moment of inertia of CHF_3. The latter was computed as a third of the trace of anisotropic tensor of the Freon, obtained at the MP2/6-31G** level of theory.

that the weight of the polarized structure φ_2 was overrated in the VB wave function when s was located in the vicinity of products. Empirically, this error could be corrected by scaling the corresponding charge density ρ_{22} (see Eq. (2.9)) before inserting it in a computation of T-matrices, namely,

$$\overline{\rho}_{22} = \gamma(s)\rho_{22}, \quad 1 \geqslant \gamma(s) > 0, \tag{7.1}$$

where scaling factor $\gamma(s)$ must decrease in the product region. In the present study, we preferred even simpler empirical prescription and scaled the computed T-matrices. Actually, it was found sufficient to fit a single matrix element $T_{22,22}^{(\infty)}$ (the equilibrium inertialess solvation energy of the polarized VB structure) by properly changing constant term A_0 in its interpolation formula (Table 3). After this correction, a reasonable shape of LEPS-3 for ABC was obtained (Table 4).

7.3. Basic unsolved problems in constructing LEPS-3 and FES-2

There exist at least two reasons underlying a breakdown of a straightforward VB computation of LEPS-3 and enforcing one to fit empirically the reorganization parameter $T_{22,22}^{(\infty)}$. Most obviously, adding a third structure with a properly smeared charge distribution to a two-state VB expansion could provide a flexibility needed to come out with an energy surface having more or less symmetric arrangement of reactant and product wells, as expected for chemical systems in which PT really occurs. The second reason to be mentioned is a lack of geometry optimization of the full solute system during a VB/PM3 computation of its charge densities ρ_{11}, ρ_{22} (Eq. (2.9)), corresponding to the two VB structures, as functions of s and R. Our tests have shown that the polarization of the second (polarized) VB structure could be smeared significantly on a relaxed solute geometry. Thereby, the effect of exaggerate solvation in the product state could be reduced even within the two-state VB treatment. Incorporation of appropriate modifications, allowing for these two reasons, in the present VB treatment, could make it more internally consistent at the expense of a significant complication of a computation scheme.

A final comment regards a computation of FES-2. The resulting energy barrier ($\sim$1 kcal/mol) obtained from a specially fitted LEPS-3 with the barrier height of $\sim$7 kcal/mol, seems to be too low. The fact of lowering the FES-2 barrier is in accord with previous computations for a different PT system [45]. The most reasonable explanation of this deficiency is a severe oversimplification brought in by substituting a real multi-dimensional PT system by a three-center model (1.1) without internal structure. An attempt to go beyond this limitation in describing the electronic structure of the solute is the main objective of the present study; the problem repeats, however, at the nuclear level. In many real PT systems, a strong geometrical distortion of the reaction center (the hybridization changes) is expected. The changes of relevant internal coordinates contribute significantly to the reaction barrier; this contribution must be eliminated prior to constructing LEPS-3 surface spanned by coordinates R, s of the three-center model. Otherwise, tunneling effects introduced at the stage of transforming LEPS-3 into FES-2, are strongly exaggerated. Finally, the

hybridization contribution must be returned and added to the FES-2 barrier. A consistent treatment of this sort is now reported [61]. Although hybridization effects are less important in the N···H···N reaction center of the present ABC system than in the C···H···C and N···H···C reaction centers considered in Refs. [45,61], still several kcal/mol could be lost when computing a barrier height according to the present simplified method.

8. Conclusion

In the present study, we extended a two-state VB treatment of PT reactions in solution. The electronic structure of two VB basis functions have been considered explicitly, based on PM-3 computations of a real many-electron reacting solute system and its fragments. The results were implemented to compute, as functions of basic PT coordinates R and s, the reorganization and solvation energies characterizing the redistribution of charge which accompanies a PT process. By this means, the incorporation of collective medium mode Z as a third essential coordinate of a PT can be consistently performed.

As usually, the two-dimensional gas-phase PES has been obtained by empirically fitting parameters of the LEPS function. Empirical fitting could not also be avoided at the stage of introducing the medium coordinate. Otherwise, the expected shapes of the important potential profiles for the three-dimensional FES (LEPS-3) could not be reproduced. Ideally, a procedure of constructing LEPS-3 would appear as follows. At first, a two-dimensional potential function is empirically calibrated in order to reproduce as closely as possible the shape of the gas-phase PES which is verified independently by high level quantum-chemical computations and by the experiment. The second stage, including the incorporation of the medium coordinate in terms of the present scheme, should be free of adjustable parameters. We failed to satisfy these conditions on both stages. The question whether such ideal scheme can be realized in the framework of a two-state model VB Hamiltonian remains open.

For two different test systems, we have studied the dependencies of basic parameters controlling the shape of LEPS-3 (the resonance and overlap integrals between VB structures, the reorganization and solvation energies) as functions of R and s. Their changes can be modeled by simple smooth functions, but the character of changes strongly depends on a particular PT system. Finally, for the ABC system we performed quantum-mechanical averaging LEPS-3 over proton coordinate s resulting in a pair of two-dimensional surfaces (FES-2) which control the dynamics of heavy coordinates R and Z. The nonadiabatic coupling parameter between these two surfaces was tentatively estimated. Based on this computation we expect that the reaction proceeds adiabatically (low potential barrier, relatively large energy gap) which seems to be in accordance with small H/D isotope effect observed experimentally for this system. Studies of temperature dependence of the rate constant seem to be more problematic because of methodological problems inherent to the continuum solvation approach [42].

Acknowledgements

The research was made possible in part by the International Association for the Promotion of Cooperation with Scientists from the New Independent States of the Former Soviet Union (project INTAS-RFBR IR-97-620). The authors also acknowledge financial support from Russian Foundation for Fundamental Research (Projects No. 96-15-97465 and 99-03-33196). One of the authors (M.V.V) is grateful to the Alexander von Humboldt foundation for the financial support of his stay in Berlin, Germany, where the final stage of preparation of the manuscript was completed.

Appendix A. The reduction of the free energy to a one-dimensional form in the solvent coordinate space

The derivation of expression (3.15) for the one-dimensional (relative to medium coordinates) FES $U(Z)$ is based on an introduction of shifted medium variables [33]:

$$X_{ab} = Y_{ab} + T_{11,ab}. \tag{A.1}$$

After changing the variables similar to the change $Y_{ab} \to Z_{ab}$ (3.10), but now for the shifted representation (A.1), we get a pair of coordinates

$$\begin{aligned} &X_{11} = Z_{11} + T_{11,11}, \\ &X \equiv X_{22} - X_{11} = Z + T_{11,22} - T_{11,11}. \end{aligned} \tag{A.2}$$

In terms of coordinates (A.2), with a vector notation

$$\left\langle\left\langle \bar{\bar{x}} \right| = (X_{11}, X), \tag{A.3}$$

the following relation is valid (see Eqs. (6.1) of Ref. [33]):

$$\begin{aligned} U(X_{11}, X) = \overline{W} - \frac{1}{2} T'_{11,11} \\ + \frac{1}{2} \left\langle \left\langle \bar{\bar{x}} \right| \left(T'\right)^{-1} \left| \bar{\bar{x}} \right\rangle \right\rangle, \end{aligned} \tag{A.4}$$

where matrix T' is defined by Eq. (3.11). We use finally the identity (Ref. [33, formulae (6.8)]):

$$\frac{1}{2} \left\langle \left\langle \bar{\bar{x}} \right| \left(T'\right)^{-1} \left| \bar{\bar{x}} \right\rangle \right\rangle = \frac{1}{2T'_{22,22}} X^2. \tag{A.5}$$

On inserting in Eq. (A.4), it results in our basic FES Eq. (3.15). An essential note is that the identity (A.5) is true only at the stationary points ($\partial U / \partial Y_{ij} = 0$) of a multi-dimensional FES.

The present derivation could make an impression that, in some sense, variables X are more convenient for FES calculations. This is indeed so when medium coordinates are the only FES variables, as in the case of electron transfer processes [33,34]. In the present PT case, when solute variables R, s cannot be ignored, all "constants" in Eqs. (A.1)–(A.4) become (R, s)-dependent. When they are included in a definition of a variable as in Eq. (A.2), the corresponding FES acquires undesirable properties (for instance, it loses obvious symmetry properties for symmetric PT systems [16]). This is why working with more fundamental variables Y_{aa} and Z_{aa} seems preferable.

Appendix B. Evaluation of the coupling matrix element

The thermally averaged coupling element $\langle G_{12} \rangle_{\mathrm{T}}$ is written as [45]

$$\langle G_{12} \rangle_{\mathrm{T}} = \frac{\hbar}{\mathrm{i}} \sqrt{\frac{2k_{\mathrm{B}}T}{\pi}} \left[\frac{J_{\mathrm{R}}}{\sqrt{\mu_{\mathrm{R}}}} + \frac{J_y}{\sqrt{\mu_y}} \right], \tag{B.1}$$

where μ_y is the mass corresponding to the effective medium coordinate y, see below, and μ_{R} is a reduced mass of heavy molecular fragments $\mathrm{R_A}$ and $\mathrm{R_B}$. The value of μ_{R} is equal to 28 amu. Matrix elements J_{R} and J_y are expressed in terms of the LEPS-3 $U(s,R,Z)$ as

$$J_{\mathrm{R}} = \frac{\left\langle \chi_2 \left| \frac{\partial U}{\partial R} \right| \chi_1 \right\rangle}{\Delta} \quad \text{and} \quad J_y = \frac{\left\langle \chi_2 \left| \frac{\partial U}{\partial y} \right| \chi_1 \right\rangle}{\Delta}. \tag{B.2}$$

Here χ_1 and χ_2 are the proton wave functions obtained by solving s-dependent Schrödinger equation [45], when two "heavy" coordinates are fixed at their values corresponding to the TS point on the FES-2.

The coordinate y relates to the coordinate Z via the following equation [45]:

$$y = \frac{Z}{\sqrt{2f_0 E_{\mathrm{r}}}}. \tag{B.3}$$

Here E_{r} is the reorganization energy at the TS point of the FES-2 and f_0^{-1} is the Pekar factor:

$$f_0^{-1} = \frac{1}{4\pi} \left(\frac{1}{\varepsilon_0} - \frac{1}{\varepsilon_\infty} \right) \tag{B.4}$$

with ε_0 and ε_∞ being the dielectric constants of the polar solvent.

In order to calculate μ_y, one has to know ε_0, ε_∞ and Debye period τ at a given temperature [16]. However, the τ value is not available for Freons. It was estimated from the viscosity of bromoethane, using the conventional expression:

$$\tau = \frac{3V\eta}{k_{\mathrm{B}}T}, \tag{B.5}$$

where V is the volume of the solvent molecule and η is viscosity of the solvent at a given temperature. We choose bromoethane, since its viscosity at low

temperatures (around 160 K) is similar to those of Freons. On the other hand, viscosity data within a wide temperature range are available for bromoethane, see Table 2.2 in Ref. [62]. These data enable us to extrapolate τ to low temperatures from the experimental value at room temperature [63] using Eq. (B.5). The experimental values of τ and η for bromoethane, used for a computation down to 160 K (the melting point of bromoethane) are given in Table 5 which also contains other data pertaining to this calculation. The resulting value $\tau = 7 \times 10^{-11}$ s was used as a Debye period for the evaluation of the mass of Freon at 110 K which was performed as described in the appendix in Ref. [16]. It was supposed that Freon can be treated in terms of a Debye spectrum of dielectric losses with a truncated tail.

The values of parameters, appearing in this appendix, are given in Tables 2, 4 and 5 and in Section 6.4.

References

[1] R.P. Bell, The Proton in Chemistry, Chapman and Hall, London, 1973.
[2] R.R. Dogonadze, A.M. Kuznetsov. The Kinetics of Chemical Reactions in Polar Solvents. The Advances in Science and Techniques, 1973, VINITI, Moscow (in Russian).
[3] J. Ulstrup, Charge Transfer Processes in Condensed Media, Springer, Berlin, 1979.
[4] A.M. Kuznetsov, Charge Transfer in Physics, Chemistry and Biology: Physical Mechanisms of Elementary Processes and introduction to the theory, Gordon and Beach Science, Reading, MA, 1995.
[5] J.K. Hwang, Z.T. Chu, A. Yadav, A. Warshel, J. Phys. Chem. 95 (1991) 8445.
[6] D. Borgis, G. Tarjus, H. Azzouz, J. Phys. Chem. 96 (1992) 3188.
[7] D. Borgis, G. Tarjus, H. Azzouz, J. Chem. Phys. 97 (1992) 1390.
[8] A. Staib, D. Borgis, J.T. Hynes, J. Chem. Phys. 102 (1995) 2487.
[9] L. Lobaugh, G.A. Voth, J. Chem. Phys. 100 (1994) 3039.
[10] D. Laria, G. Ciccoti, M. Ferrario, R. Kapral, J. Chem. Phys. 97 (1992) 378.
[11] J. Mavri, H.J.C. Berendsen, W.F. van Gunsteren, J. Phys. Chem. 97 (1993) 13469.
[12] J. Mavri, H.J.C. Berendsen, J. Phys. Chem. 99 (1995) 12711.
[13] S. Hammes-Schiffer, J.C. Tully, J. Chem. Phys. 101 (1994) 4657.
[14] A. Warshel, Computer Modeling of Chemical Reactions in Enzymes and Solution, Wiley, New York, 1993.
[15] A. Warshel, J.K. Hwang, J. Chem. Phys. 84 (1986) 4938.
[16] M.V. Basilevsky, A.V. Soudackov, M.V. Vener, Chem. Phys. 200 (1995) 87.
[17] E. Cances, B. Mennucci, J. Tomasi, J. Chem. Phys. 109 (1998) 2798.
[18] M.F. Ruiz-Lopez, A. Oliva, I. Tunon, J. Bertran, J. Phys. Chem. A 102 (1998) 10728.
[19] D. Borgis, S. Lee, J.T. Hynes, Chem. Phys. Lett. 162 (1989) 19.
[20] D. Borgis, J.T. Hynes, Chem. Phys. 170 (1993) 315.
[21] D. Borgis, J.T. Hynes, J. Phys. Chem. 100 (1996) 1118.
[22] C.A. Mead, D.G. Truhlar, J. Chem. Phys. 77 (1982) 260.
[23] U.W. Schmitt, G.A. Voth, J. Phys. Chem. B 102 (1998) 5547.
[24] R. Vuilleumier, D. Borgis, J. Chem. Phys. 111 (1999) 4251.
[25] A. Warshel, R.M. Weiss, J. Am. Chem. Soc. 102 (1980) 6218.
[26] S. Miertus, E. Scrocco, J. Tomasi, Chem. Phys. 55 (1981) 117.
[27] J. Tomasi, M. Persico, Chem. Rev. 24 (1994) 2027.
[28] M.V. Basilevsky, G.E. Chudinov, Chem. Phys. 157 (1991) 327.
[29] M.V. Basilevsky, I.V. Rostov, M.D. Newton, Chem. Phys. 232 (1998) 189.
[30] M.D. Newton, I.V. Rostov, M.V. Basilevsky, Chem. Phys. 232 (1998) 201.
[31] M.V. Basilevsky, G.E. Chudinov, Chem. Phys. 157 (1991) 345.
[32] M.V. Basilevsky, G.E. Chudinov, J. Mol. Struct. (THEOCHEM) 260 (1992) 223.
[33] M.V. Basilevsky, G.E. Chudinov, M.D. Newton, Chem. Phys. 179 (1994) 263.
[34] M.V. Basilevsky, I.V. Rostov, M.D. Newton, J. Electroanal. Chem. 450 (1998) 69.
[35] J. Kim, J.T. Hynes, J. Chem. Phys. 93 (1990) 5194.
[36] H.J. Kim, J.T. Hynes, J. Chem. Phys. 96 (1992) 5088.
[37] R. Bianco, J.T. Hynes, J. Chem. Phys. 102 (1995) 7864.
[38] R. Bianco, J.T. Hynes, J. Chem. Phys. 102 (1995) 7885.
[39] P. Kuntz, in: W.H. Miller (Ed.), Dynamics of Molecular Collisions, Part B, Plenum Press, New York, 1976 (Chapter 2).
[40] R. McWeeny, B.T. Sutcliffe, Methods of Molecular Quantum Mechanics, Academic Press, New York, London, 1976.
[41] P.O. Löwdin, Phys. Rev. 97 (1955) 1474.
[42] I.V. Rostov, M.V. Basilevsky, M.D. Newton, in: L.R. Pratt, G. Hummer (Eds.), Simulation and Theory of Electrostatic Interactions in Solution, American Institute of Physics, 1999, p.331.
[43] M.V. Basilevsky, G.E. Chudinov, Chem. Phys. 165 (1992) 213.
[44] H.J. Kim, R. Bianco, B.J. Gertner, J.T. Hynes, J. Phys. Chem. 97 (1993) 1723.

[45] M.V. Basilevsky, M.V. Vener, G.V. Davidovich, A.V. Soudackov, Chem. Phys. 208 (1996) 267.
[46] J.J.P. Stewart, J. Comp. Chem. 10 (1989) 221.
[47] N.S. Golubev, V.I. Faustov, M.V. Vener, B. Mennucci, in preparation.
[48] R. Vuilleumier, D. Borgis, Chem. Phys. Lett. 284 (1998) 71.
[49] M.D. Newton, J. Chem. Phys. 67 (1977) 5535.
[50] L. Olamae, I. Schavitt, S.J. Singer, Int. J. Quant. Chem. Symp. 29 (1995) 657.
[51] M.V. Vener, J. Sauer, Chem. Phys. Lett. 312 (1999) 591.
[52] N.B. Librovich, V.P. Sakun, N.D. Sokolov, Chem. Phys. 60 (1981) 425.
[53] D.E. Sagnella, M.E. Tuckerman, J. Chem. Phys. 108 (1998) 2073.
[54] U.W. Scmitt, G.A. Voth, J. Chem. Phys. 111 (1999) 9361.
[55] M.D. Newton, N. Sutin, Ann. Rev. Phys. Chem. 35 (1984) 437.
[56] A.C. Legon, Chem. Soc. Rev. 22 (1993) 153.
[57] A. Iwasaki, M. Fujii, T. Watanabe, T. Ebata, N. Mikami, J. Phys. Chem. 100 (1996) 16053.
[58] T. Rospenk, T. Zeegers-Huyskens, J. Phys. Chem. A 101 (1997) 8428.
[59] M.V. Vener, Chem. Phys. Lett. 244 (1995) 125.
[60] J.E. Del Bene, M.J.T. Jordan, J. Chem. Phys. 108 (1998) 3205.
[61] V.A. Tikhomirov, A.V. Soudackov, M.V. Basilevsky, J. Phys. Chem. A, in press.
[62] J.A. Riddick, W.B. Bunger, T.K. Sakano, Organic Solvents. Physical Properties and Methods of Purification, fourth ed., Wiley, New York, 1986.
[63] M.F. Fux, Electric and Optical Properties of Molecules and Condensed Media, Leningrad University Publishers, Leningrad, 1984 (in Russian).